BIOCHEMISTRY
including biophysical chemistry & molecular biology

Article

pubs.acs.org/biochemistry

Characteristics of Halorhodopsin–Bacterioruberin Complex from *Natronomonas pharaonis* Membrane in the Solubilized System

Takanori Sasaki,* Nur Wahida Abdul Razak, Noritaka Kato, and Yuri Mukai

School of Science and Technology, Meiji University, Tama-ku, Kawasaki-shi, Kanagawa 214-8571, Japan

ABSTRACT: Halorhodopsin is a retinal protein with a seven-transmembrane helix and acts as an inward light-driven Cl^- pump. In this study, structural state of the solubilized halorhodopsin (NpHR) from the biomembrane of mutant strain KM-1 of *Natronomonas pharaonis* in nonionic detergent was investigated. A gel filtration chromatography monitored absorbances at 280 and 504 nm corresponding to the protein and a lipid soluble pigment of bacterioruberin (BR), respectively, has clearly detected an oligomer formation of the NpHRs and a complex formation between the NpHR and BR in the solubilized system. A molar ratio of NpHR:BR in the solubilized complex was close to 1:1. Further SDS-PAGE analysis of the solubilized NpHR cross-linked by 1% glutaraldehyde has revealed that the NpHR forms homotrimer in detergent system. Although this trimeric structure was stable in the presence of NaCl, it was dissociated to the monomer by the heat treatment at 45 °C in the desalted condition. The same tendency has been reported in the case of trimeric NpHR expressed heterologously on the *E. coli* membrane, leading to a conclusion that the change of strength of the trimeric association dependent on the ion binding is a universal feature of the NpHR. Interestingly, the trimer dissociation on the NpHR was accompanied by the complete dissociation of the BR molecule from the protein, indicated that the cavity formed by the NpHR protomers in the trimeric conformation is important for tight binding of the BR. Because the binding affinity for Cl^- and the resistance to hydroxylamine under light illumination showed only minor differences between the NpHR in the solubilized state and that on the biomembrane, the influences of solubilization to the tertiary structure and function of the protein are thought to be minor. This NpHR–BR complex in the solubilized system has a potential to be a good model system to investigate the intermolecular interaction between the membrane protein and lipid.

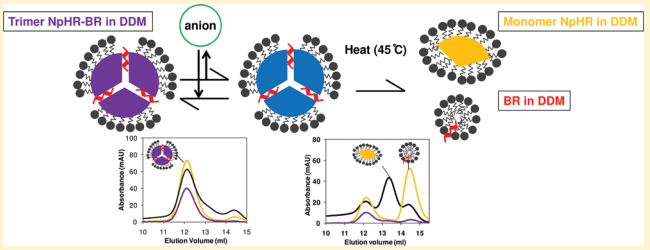

Seven transmembrane proteins (7TMs) which contain G protein-coupled receptors and eubacterial/archaeal rhodopsins are involved in many biological processes by mediating signal transduction or pumping ions across the plasma membrane. The functions and conformations of these proteins are modulated by the oligomeric associations, and many kinds of GPCRs are known to modify those signaling and trafficking by the homo- or heterodimerization.[1,2] Light-driven proton pump bacteriorhodopsin (bR), one of the archaeal rhodopsins, also forms the homotrimer and changes its structure photocooperatively between the neighboring proteins.[3,4]

It is also reported that interactions between 7TMs and lipids control the structure and functional efficiency of those proteins. Taking the rhodopsin of a GPCR as an example, the binding of the docosahexanoic acid acyl chain (DHA) destabilizes the protein structure and enhances the kinetics of the photocycle.[5,6] Some specific rhodopsin–DHA binding sites also have been proposed from the experiments and molecular dynamics simulations.[7,8] In the case of xanthorhodopsin of *Salinibacter ruber*, a carotenoid of salinixanthin bound to the protein is known to function as a light-harvesting antenna for supplying additional excitation energy for retinal isomerization and proton transport.[9−11] However, only a few model proteins offer detailed information on the functional/structural effects by the interaction between 7TM and lipid. Notably, the bound lipids are often dissociated from the protein in the solubilized system although this system has some advantages for analysis, for instance, the low turbidity of the solution and the high purity of the sample with roughly equal size.

Halorhodopsin from *Natronomonas pharaonis* (NpHR), one of the 7TMs, is a light-driven anion pump[12,13] and a heterologous expression system in *Escherichia coli* has been established on this protein.[14] Fortunately, NpHR can form trimer in the cell membrane of *E. coli* and retains its oligomeric form even after solubilization by nonionic detergent in the presence of salt.[15] So this trimer NpHR in detergent has been utilized to quantify the association energy of oligomer[16] and identify the amino acid residue essential to form/retain the trimer,[17] contributing to the studies on the oligomerization mechanism of the archaeal rhodopsins. Recently, Kouyama et al. have reported the X-ray crystal structure of NpHR obtained directly from the hR-overproducing mutant strain KM-1 of the *N. pharaonis* ($DSM2160^T$).[18,19] In this structure, a lipid soluble pigment (carotenoid) of bacterioruberin (BR) binds to crevices between adjacent protein subunits in the trimeric assembly, in contrast to the trimeric NpHR obtained from *E. coli* system which does not bind the carotenoid (Figure 1). However, it is still in debate whether this protein–carotenoid complex on the biomembrane

Received: December 19, 2011
Revised: February 27, 2012
Published: February 28, 2012

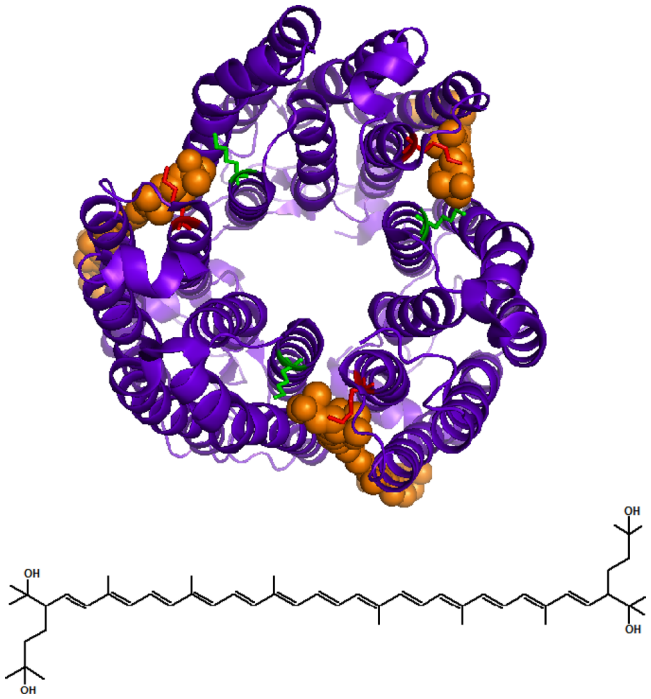

Figure 1. Upper: trimer model of NpHR from PDB file 3A7K. The NpHR and BR molecules were colored by purple and orange, respectively. K65 and K148, which are the targets for cross-linking by glutaraldehyde, are shown in green and red, respectively. A view into the membrane plane is seen from the cytoplasmic side of the membrane. Lower: chemical structure of a carotenoid of BR.

has been kept in the solubilized system and whether it is possible to study on the protein−carotenoid interaction in the solubilized system as a pseudoenvironment of the biomembrane.

In this study, the characterisitics of the solubilized NpHR from the biomembrane of mutant strain KM-1 were investigated by using nonionic detergent, *n*-dodecyl *β*-D-maltopyranoside (DDM) and Triton X-100. Solubilized components of the NpHR and BR were confirmed to form a complex in a detergent micelle by a gel filtration chromatography monitored absorbances at 280 and 504 nm, corresponding to the protein and BR, respectively. Further analyses by the gel filtration chromatography, SDS-PAGE, and UV/vis absorption spectroscopy have revealed that the NpHR retains a homotrimer and can bind the BR with molar ratio of NpHR:BR = 1:1 even in the solubilized system. Although this complex was stable in the presence of NaCl, dissociations not only of the NpHRs but also of the BR from the complex were caused in the absence of NaCl by the heat treatment at 45 °C. These results indicate that ion binding to the NpHR is important for the stabilization of the complex and that the cavity formed by the NpHR protomers in the trimer is essential to the tight binding of the BR. Because the influences of solubilization on the structural features of the NpHR like the anion binding affinity and the resistance to hydroxylamine were minor, the NpHR−BR complex in the solubilized system is suitable to investigate the specific intermolecular interaction between the membrane protein and lipid conveniently.

MATERIALS AND METHODS

Preparation of *N. pharaonis* Cell Membrane and Solubilized NpHR−BR Complex. Membrane of *N. pharaonis* strain KM-1 (DSM2160^T) was prepared as described previously.[20] Briefly, the cells were grown at 37 °C for two weeks under light illuminated condition in the culture medium (pH 9.0) contained: 1 g KH_2PO_4, 1 g KCl, 1 g NH_4Cl, 200 mg $MgSO_4{\cdot}7H_2O$, 200 g NaCl, 1 g monosodium glutamate, 5 g casamino acids, 5 g yeast extract, 15 g Na_2CO_3, and trace metals (1 μL HCl (32%), 0.2 mg $FeCl_2{\cdot}4H_2O$, 0.025 mg $CoCl_2{\cdot}6H_2O$, 0.01 mg $MnCl_2{\cdot}4H_2O$, 7 μg $ZnCl_2$, 0.6 μg H_3BO_3, 4 μg $Na_2MoO_4{\cdot}2H_2O$, 7 μg $NiCl_2{\cdot}6H_2O$, 0.2 μg $CuCl_2{\cdot}2H_2O$, 2.5 μg $AlCl_3$, 0.6 μg $Na_2WO_4{\cdot}2H_2O$, 2.5 μg $AlCl_3$, 0.6 μg $Na_2WO_4{\cdot}2H_2O$). Cells were collected by centrifugation and suspended in the culture medium without monosodium glutamate, casamino acids, and yeast extract. After DNase treatment for 24 h at room temperature and three cycles of freeze−thaw, the suspension was centrifuged at 10000*g* for 15 min at 4 °C to remove undisrupted cells. The obtained cell membranes were washed three times with 2 M KCl, eight times with distilled water, and once with 10 mM Tris-HCl buffer (pH 7.0) contained 0.5−1.0% (w/v) Tween 20 and 0.1 M NaCl to remove the excess BR molecules on the membrane.

The NpHR−BR complex in cell membrane was solubilized by *n*-dodecyl *β*-D-maltopyranoside (DDM) (Dojindo Lab, Kumamoto, Japan) or Triton X-100 (Wako, Osaka, Japan) in 0.1% MOPS buffer (pH 7.0), 150 mM NaCl at 25 °C for 24 h. The sample solution was centrifuged at 142000*g* for 30 min at 4 °C, and the supernatant was regarded as the solubilized NpHR−BR complex. When controlling for NaCl concentration, the sample solution was once desalted by passage over Sephadex-25 in a PD-10 column (8.3 mL; Amersham Pharmacia Biotech, Uppsala, Sweden) in 0.1% MOPS buffer (pH 7.0) containing 0.1% DDM.

Expression and Purification of Trimeric NpHR in *E. coli* Expression System. Expression and purification procedure for the histidine-tagged NpHR using *E. coli* BL21(DE3) cells harboring the plasmid were performed by the methods described previously.[14] *E. coli* membrane was solubilized by 30 mM DDM and a fraction of NpHR was collected with Ni-NTA agarose (Qiagen, Hilden, Germany) with 50 mM Tris-HCl (pH 7.0), 300 mM NaCl, 2 mM DDM, and 150 mM imidazole. The protein concentration in the presence of Cl^- was estimated using an extinction coefficient ε_{578} of 54 000 M^{-1} cm^{-1}.[21] Monomerized NpHR in DDM was prepared by heat treatment at 40 °C for 24 h in the absence of NaCl.

Preparation of bR from *H. salinarum*. Purple membrane of *H. salinarum* strain R1M1 contained bR was prepared according to the method of Oesterhelt and Stoekenius.[22] The purified samples were suspended in 5 mM Tris-HCl buffer (pH 7.0). The concentration of bR in purple membrane was determined from absorption maximum at 568 nm using an extinction coefficient of 62 700 M^{-1} cm^{-1}.[23]

Spectroscopic Measurements. Absorption spectra were recorded on a S-3100 UV−vis spectrophotometer (SCINCO, Seoul, Korea). The obtained spectral data were analyzed using Peakfit (Seasolve Software Inc., Framingham, MA) software.

Gel Filtration Chromatography. Gel filtration chromatography of the DDM (or Triton X-100) solubilized NpHR and NpHR-BR complex was performed by ÄKTA purifier chromatography system (GE Healthcare, Uppsala, Sweden). The sample (150 μL) was applied to a Superdex 200 10/300 GL size exclusion column (total bed volume [V_t] = 24 mL) (GE Healthcare, Uppsala, Sweden) that had been equilibrated previously with 50 mM NaPi (pH 7.0), 150 mM NaCl, and 0.1% DDM. The column was run at a flow rate of 800 μL/min, and protein and BR eluted were monitored at 280, 504, and 578 nm. Standard proteins for calibration of the molecular mass

were thyroglobulin (669 kDa), ferritinn (440 kDa), aldolase (158 kDa), conalbumin (75 kDa), and ovalbumin (44 kDa). The excluded volumes (V_0) were determined using blue dextran. All samples were chromatographed at 25 °C. To prepare a calibration curve of K_{av} values versus log molecular weight, the K_{av} of each protein was calculated according to the equation

$$K_{av} = (V_e - V_0)/(V_t - V_0)$$

where V_e is the elution volume for the protein.

SDS-PAGE. Cross-linked NpHR oligomer sample for SDS-PAGE was prepared by addition of 1% glutaraldehyde (Wako, Osaka, Japan) and incubation at 35 °C for 30 min in 10 mM MOPS buffer (pH 7.0) containing 0.1% DDM. The appropriate amount of sample and 2X loading buffer (100 mM Tris-HCl pH 6.8, 20% glycerol, 2% SDS, 0.2% bromophenol blue) were mixed. Samples were loaded on a 12% precast polyacrylamide gel (Bio-Rad Laboratories, Hercules, CA). As a standard, protein molecular weight marker (broad) (Takara, Otsu, Japan) was also loaded. The gel was electrophoresed at 200 V for 25 min and staind with silver.

BR Titration Experiment for Trimeric NpHR. The BR for titration experiment was purified from the *N. pharaonis* membrane. Briefly, 95% methanol was added to the membrane pellet, and the suspension was sonicated twice on ice by the homogenizer VP-050 (Taitec, Nagoya, Japan) for 30 s. After incubation for 12 h at −20 °C, the suspension was centrifugated at 2000*g* for 5 min, and the supernatant containing the extracted BR was transferred to a new Eppendorf tube. The supernatant was immediately evaporated on a rotary vacuum pump (VC-15SP) (Taitec, Nagoya, Japan) and resuspended to acetone. After centrifugation at 15000*g* for 1 min, the supernatant was used for titration experiment.

For titration experiment, each volume of acetone solution contained BR was dried by a nitrogen flow, and the pellets were suspended in 300 μL of 10 mM MOPS buffer with 6 μM NpHR solubilized from the *E. coli* membrane, 150 mM NaCl, and 0.1% DDM (pH 7.0). Final concentrations of the BR in suspensions were 1, 2, 3, 4, 5, 6, 8, 10, and 15 μM, respectively. After incubation for 3 h at 25 °C, the suspensions were applied to the gel filtration chromatography. To quantify the unbound BR molecules to the NpHR, the gel filtration chromatography monitored at 504 nm was also performed for 0.1% DDM solutions contained each concentration of BR (0, 0.5, 1, 2, 3, 4, and 5 μM), followed by generation of a standard curve. Because the peak area of the BR in DDM with a peak at 14.5 mL was proportional to the BR concentration, the linear curve was obtained.

Bleaching Measurement in the Presence of Hydroxylamine. The NpHR or bR sample solutions before and after solubilization by detergents were mixed with the hydroxylamine, respectively. Then the sample solutions were incubated at 25 °C under continuous illuminated conditions. Bleaching of the proteins was monitored by absorbance change at around 578 nm in the case of NpHR and around 560 nm in the case of bR for 30−60 min. A 150 W halogen lamp illuminator equipped with a sharp cut filter Y-52 and a light control was used as a light source. All bleaching curves obtained could be expressed as a single-exponential decay function, which was used to determine the rate constants of photobleaching.

RESULTS

Spectroscopic Features of NpHR Solubilized from *N. pharaonis* Membrane. Figure 2A shows the absorption spectra of the purified *N. pharaonis* membrane (solid line), solubilized component from this membrane (dashed line), and the precipitated component (dotted line) after solubilization by 20 mM DDM. Almost 85% of the NpHRs with an absorption peak at 578 nm in the presence of NaCl were solubilized. The solubilized component also had the absorption band with peaks at 474, 504, and 540 nm corresponding to the BR, and the absorption peak ratio of $Abs_{578\ nm}$:$Abs_{504\ nm}$ was about 1:2.2. DDM concentration dependencies for solubilization ratios (Figure 2B) show that the solubilization ratios of both the NpHR and the BR reached a plateau of about 85% at around 5 mM DDM. NpHR was also solubilized stably by Triton X-100 with higher solubilization ratios than that by DDM in the low

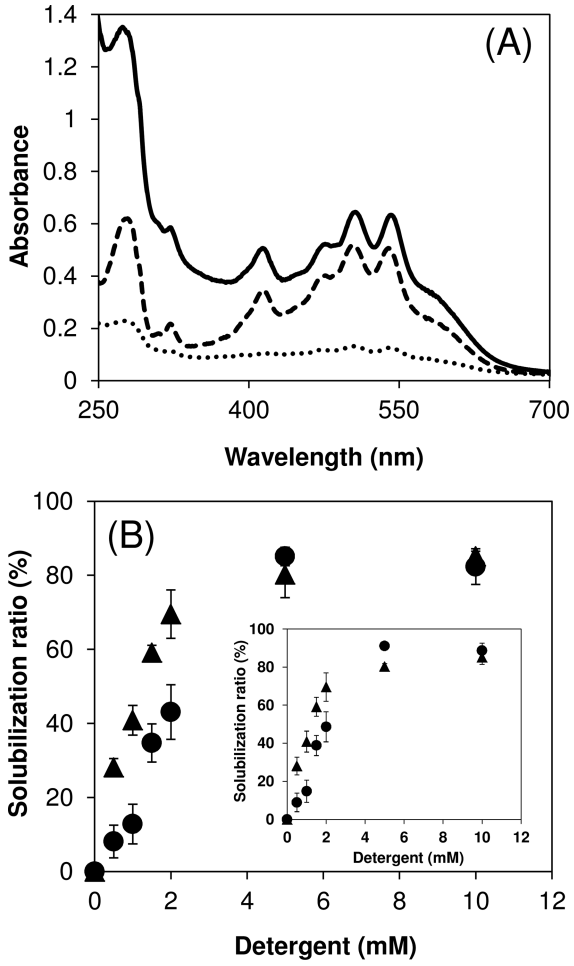

Figure 2. (A) Absorption spectra of the *N. pharaonis* membrane (solid line), the supernatant (dashed line), and the precipitate (dotted line) after solubilization treatment by 20 mM DDM at 25 °C for 24 h and centrifugation. (B) Detergent concentration dependencies for solubilization ratios of NpHR from *N. pharaonis* membrane by DDM (circles) and Triton X-100 (triangles) calculated from the absorbances at 578 nm. Inset: detergent concentration dependencies for solubilization of BR by DDM (circles) and Triton X-100 (triangles) calculated from the absorbances at 504 and 509 nm, respectively. Average values ± standard deviation (n = 3). The solubilization treatment was performed at 25 °C for 24 h. Buffer conditions: 10 mM MOPS (pH 7.0) with 100 mM NaCl.

dx.doi.org/10.1021/bi201876p | *Biochemistry* 2012, 51, 2785−2794

detergent concentration range (Figure 2B (triangles)). In the case of the solubilized sample in Triton X-100, absorption peaks of the BR component were red-shifted by 4−5 nm compared to those of the solubilized sample in DDM (data not shown). The cooperative solubilizations of the NpHR and BR as shown in Figure 2B and its inset suggest the complex formation between the NpHR and BR.

Figure 3A,B shows the absorption spectra in the 450−700 nm range of solubilized component from *N. pharaonis* membrane by DDM in the presence of 300 mM NaCl (A) and absence of NaCl (B), respectively. The absorption spectra can be decomposed into two components: an absorption band from NpHR (dashed line) and a band from BR with notable peaks at 474, 504, and 540 nm (dotted line). On the decomposed spectra of NpHR, a blue shift of λ_{max} from 600 to 578 nm and an increase of the maximum absorbance by 1.1 times corresponding to a change in the extinction coefficient were observed by addition of NaCl, as reported previously.[21] Because almost 98% of the peak intensity at 578 nm in the presence of NaCl was from the absorption component of solubilized NpHR, it is possible to estimate the NpHR concentration approximately without decomposition of spectra and by applying an extinction coefficient of ε_{578} = 54 000 M^{-1} cm^{-1}.

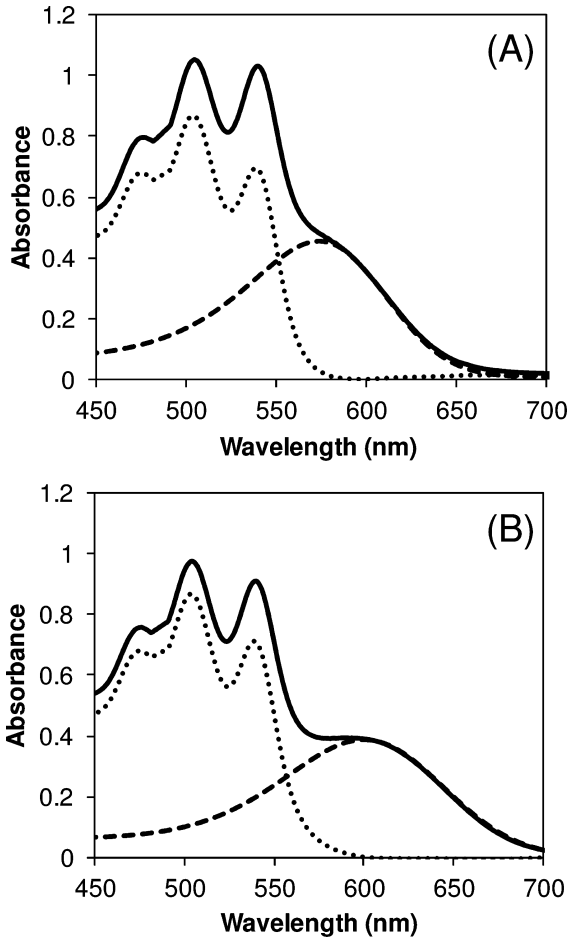

Figure 3. Absorption spectra of the solubilized NpHR and BR by DDM in the presence of 300 mM NaCl (A) and in the absence of NaCl (B). Solid line: solubilized sample from *N. pharaonis* membrane by DDM; dashed line: approximately scaled spectra of the NpHR purified from *E. coli* membrane to model the NpHR component in the solubilized sample; dotted line: BR component obtained by subtracting the spectra of the NpHR component. Buffer conditions: 10 mM MOPS (pH 7.0).

Formation of NpHR−BR Complex and Its Molar Ratio in the Solubilized System. Although the absorption spectra in Figure 3 have revealed the existence of both the NpHR and BR in the solubilized system, it was difficult to confirm the complex formation of those. So we confirmed by a gel filtration chromatography whether the solubilized NpHR forms the complex with the BR or not. Figure 4 shows the gel filtration chromatograms of solubilized component from *N. pharaonis* membrane by DDM monitored at 280, 504, and 578 nm to detect simultaneously the protein, BR, and NpHR, respectively. The main peaks of each chromatogram were all located at 12.1 mL. In addition, the area ratio of the chromatograms monitored at 578 and 504 nm with the elution peak at 12.1 mL ($Area_{578\ nm}$:$Area_{504\ nm}$) was 1:2.3, corresponding to the absorption peak ratio of $Abs_{578\ nm}$:$Abs_{504\ nm}$ = 1:2.4 estimated from the absorption spectra of solubilized NpHR−BR complex before the gel filtration (Figure 3A (solid line)). These results clearly indicate that the NpHR binds the BR tightly even after solubilization treatment.

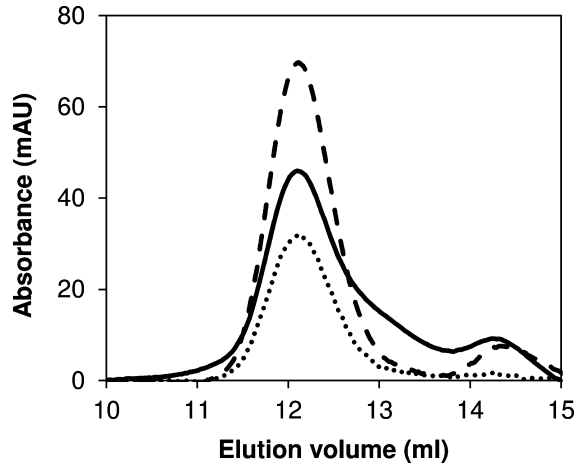

Figure 4. Gel filtration chromatogram of the solubilized NpHR sample by DDM in the presence of 300 mM NaCl. The elution profiles were monitored at 280 nm (solid line), 504 nm (dashed line), and 578 nm (dotted line). Buffer conditions for gel filtration chromatography: 50 mM NaPi (pH 7.0) with 0.1% DDM and 150 mM NaCl.

What is the molar ratio of the NpHR in detergent micelle? If an extinction coefficient of BR of ε_{496} = 187 960 M^{-1} cm^{-1} in acetone is applied to the decomposed BR spectra in Figure 3A,[24] the molar ratio of NpHR:BR in detergent micelle is estimated to be 1:0.6. This BR ratio against to the NpHR is lower than that expected from the X-ray structure of the NpHR, NpHR:BR = 1:1 (Figure 1).[18,19] In addition, based on this extinction coefficient, it is required $Abs_{578\ nm}$:$Abs_{504\ nm}$ = 1:3.5 on the absorption spectra for the complex to exist at the molar ratio of NpHR:BR = 1:1. Here, to evaluate the actual binding ratio of NpHR:BR in the solubilized complex, we performed a BR titration experiment of the NpHR expressed heterologously on the *E. coli* membrane (ENpHR), which have not bound any carotenoids. Figure 5A shows the gel filtration chromatograms monitored at 504 nm for each concentration of BR mixed with 6 μM solubilized ENpHR in DDM and incubated for 3 h. Interestingly, BR molecules were tightly bound to the ENpHR in spite of the detergent system, and the absorbance at around 12 mL (peak 1) was increased by increasing the BR concentration.

dx.doi.org/10.1021/bi201876p | *Biochemistry* 2012, 51, 2785−2794

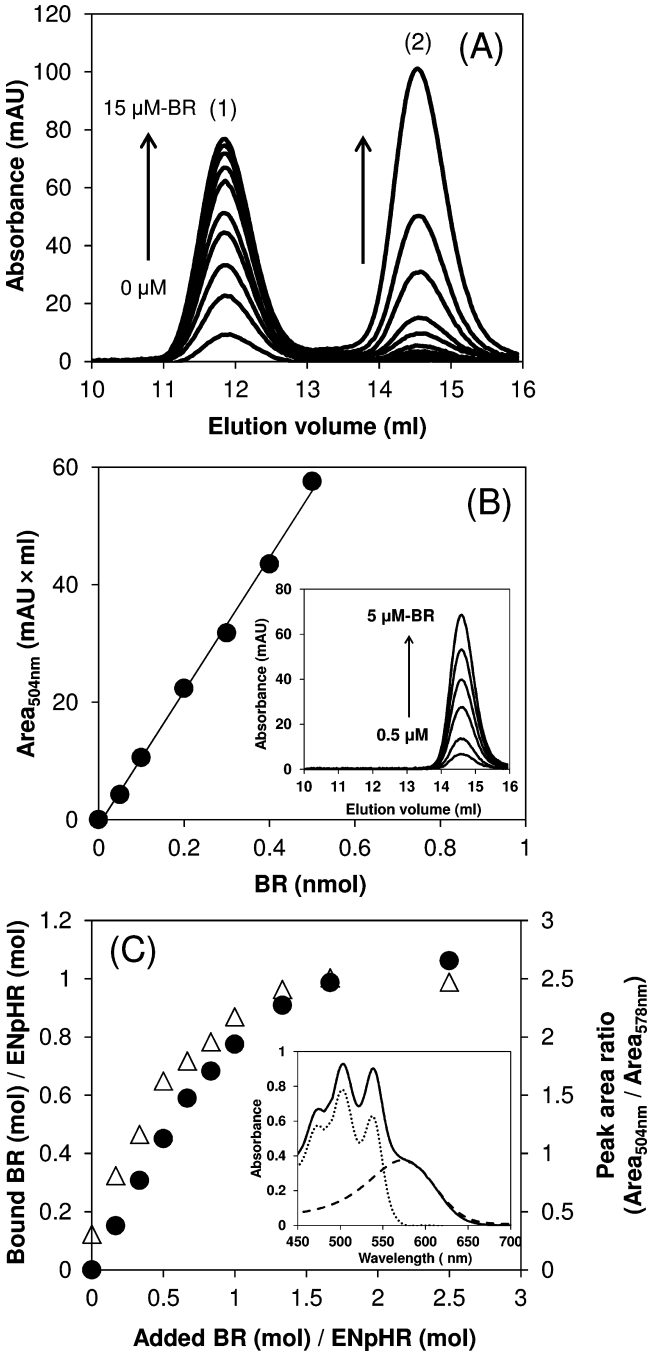

Figure 5. (A) BR titration for the solubilized ENpHR in DDM. After mixing of 0, 1, 2, 3, 4, 5, 6, 8, 10, and 15 μM of BR with 6 μM-ENpHR, the elution profiles by a gel filtration chromatography were monitored at 504 nm. Peaks 1 and 2 represent the bound and unbound BR to the ENpHR, respectively. (B) The standard curve using each number of molecules of the BR in DDM. Inset: the gel filtration chromatogram of 0.5−5 μM BR monitored at 504 nm. (C) A plot of the molar ratio of added BR to ENpHR in the sample solution versus the molar binding ratio of BR to ENpHR (circles). Open triangles: the area ratios of the chromatograms monitored at 504 nm to those at 578 nm (ENpHR component) on the peak 1 in (A). Inset: absorption spectra of the solubilized ENpHR−BR complex (molar ratio of ENpHR:BR = 1:1) after the gel filtration chromatography (solid line). Dashed line: NpHR component; dotted line: BR component.

On the other hand, the absorbance at around 14.5 mL (peak 2) was also increased. The molecular weight at this peak position was calculated to be about 60 kDa; this weight corresponds to the micelle size of DDM of about 75 kDa.[25] Considering the molecular weight of a BR to be 740, the DDM micelles containing the BR molecules which have not bound to the protein are indicated to be eluted at around 14.5 mL. Because the number of molecules of the BR in DDM had a linear correlation with the peak area of the chromatogram with elution peak at 14.5 mL, a linear standard curve was obtained (Figure 5B). By using this standard curve, we estimated the number of molecules of the unbound/bound BR to the ENpHR. As a result, it was obtained a plot of the molar ratio of the added BR to the ENpHR in the sample solution versus the molar binding ratio of the BR to the ENpHR (Figure 5C). Both the molar ratios of the BR to the NpHR in the complex (circles) and the peak area ratios of $Area_{504\,nm}$ to $Area_{578\,nm}$ (open triangles) were reached plateau of 1 and 2.5 by addition of BR molecules, which are only 1.6 times as much as ENpHR molecules. The absorption peak ratio of the solubilized complex with molar ratio of ENpHR:BR = 1:1 after the gel filtration chromatography was also $Abs_{578\,nm}$:$Abs_{504\,nm}$ = 1:2.5, corresponding to the peak area ratio (Figure 5C, inset). These results indicate that the solubilized NpHR−BR complex from *N. pharaonis* membrane which has the absorption peak ratio of $Abs_{578\,nm}$:$Abs_{504\,nm}$ = 1:2.4 (Figure 3A) has almost 1:1 of the NpHR:BR binding ratio. Probably, the extinction coefficient of the BR molecule bound to the NpHR is decreased by about 60% compared to that in acetone (that is, $\varepsilon_{504} \cong 112\,000\ M^{-1}\ cm^{-1}$ in the bound state to the protein).

Number of Oligomer Unit of NpHR in the Solubilized State. The oligomeric state of NpHR in the solubilized state was also confirmed by gel filtration chromatography. Figure 6A shows the gel filtration chromatogram monitored the absorbance at 280 nm of the solubilized component from *N. pharaonis* membrane by DDM (solid line) or Triton X-100 (dashed line). As a control, the ENpHR, which is known to keep the trimer in a detergent micelle,[15,26] was also solubilized by DDM and applied to the gel filtration chromatography (dotted line). The elution peak of the DDM−ENpHR trimer complex was located at around 11.8 mL, close to that of solubilized components from *N. pharaonis* membrane of 12.1 mL. To estimate the molecular weights of the solubilized complexes, the calibration curve with K_{av} values versus log molecular weight was constructed as shown in Figure 6B. As a result, the molecular weights of solubilized components from *N. pharaonis* membrane and DDM−ENpHR trimer complex were calculated to be 180 and 210 kDa, respectively. Considering the molecular weight of the DDM−ENpHR monomer complex (see Materials and Methods) to be 117 kDa (Figure 6A (dash-dotted line), Figure 6B (open diamond)), it is suggested that solubilized components from *N. pharaonis* have retained the oligomeric state.

To identify the number of oligomer unit of NpHR more correctly, SDS-PAGE was performed (Figure 7). In the case of trimer ENpHR, K65 of one ENpHR molecule can be cross-linked to K148 of the neighboring molecule by glutaraldehyde (GA) (Figure 1), resulting in an appearance of a trimer band in the SDS-PAGE.[15] In this study, the same trimer band was observed by cross-linking treatment to the NpHR solubilized from *N. pharaonis* membrane by DDM (Figure 7, lane NpHR +GA). Contrary to this, in the case of solubilized bacteriorhodopisn (bR) from *H. salinarum* membrane which is known to be monomerized by solubilization,[27−29] only a monomer band was observed even after cross-linking treatment (lane bR+GA). These results indicate that the solubilized NpHR

dx.doi.org/10.1021/bi201876p | *Biochemistry* 2012, 51, 2785−2794

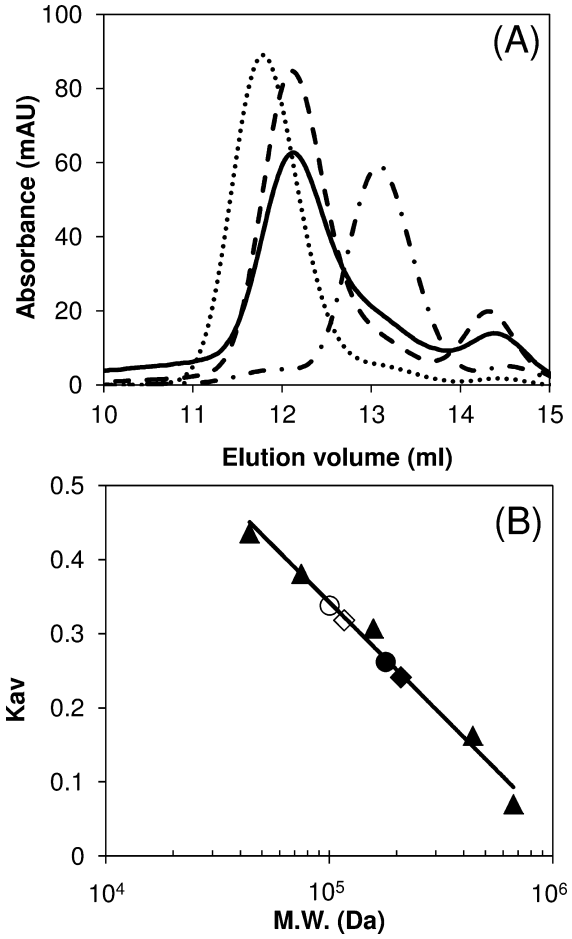

Figure 6. (A) Gel filtration chromatograms of the solubilized NpHR samples by nonionic detergents in the presence of 300 mM NaCl. The elution profiles were monitored at 280 nm. Solid line: solibilized sample by DDM; dashed line: solubilized NpHR sample by Triton X-100; dotted line: solubilized ENpHR trimer by DDM; dash-dotted line: solubilized ENpHR monomer by DDM. Buffer conditions for gel filtration chromatography: 50 mM NaPi (pH 7.0) with 0.1% DDM and 150 mM NaCl. (B) The calibration curve using the five kinds of globular protein standards (triangles). Circle: DDM–NpHR–BR complex; open circle: dissociated DDM–NpHR complex after incubation at 45 °C for 24 h in the absence of NaCl; diamond: DDM–ENpHR trimer complex; open diamond: DDM–ENpHR monomer complex.

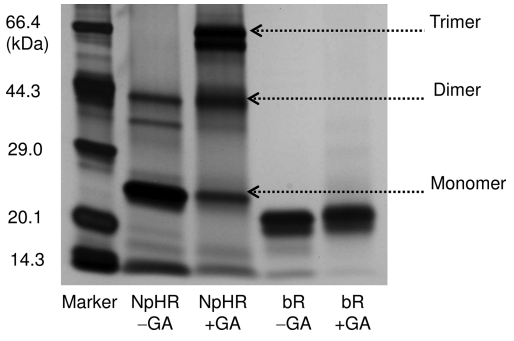

Figure 7. SDS-PAGE of solubilized NpHRs by DDM before and after cross-linking by GA. Lane marker: standard, lane No GA: NpHR without cross-linking, lane +GA: NpHR after cross-linking, lane No GA(bR): solubilized bR by Triton X-100 without cross-linking, lane +GA(bR): solubilized bR by Triton X-100 after cross-linking. Cross-linking treatment was performed with 1% GA at 35 °C for 30 min.

maintains the specific trimer conformation. Both of the monomer and trimer bands of the NpHR were positioned a bit lower than those of the theoretical molecular weights of monomer (31 kDa) and trimer (93 kDa), respectively. This is partially due to the low theoretical isoelectric point of 4.31 on this protein. In fact, as shown in lane bR-GA of Figure 7, the monomer band of bR with theoretical isoelectric point of 4.72 was also located a bit lower than of the theoretical molecular weight of 27 kDa. The trimer band of the NpHR was split into two distinct subbands although the monomer band was not. Although the reason for this has been remained unclear, two kinds of denaturated states of the cross-linked trimer NpHR in SDS may exist.

Dissociation of NpHR–BR Complex by Heat Treatment. As shown in Figure 8A, the complex composed of the

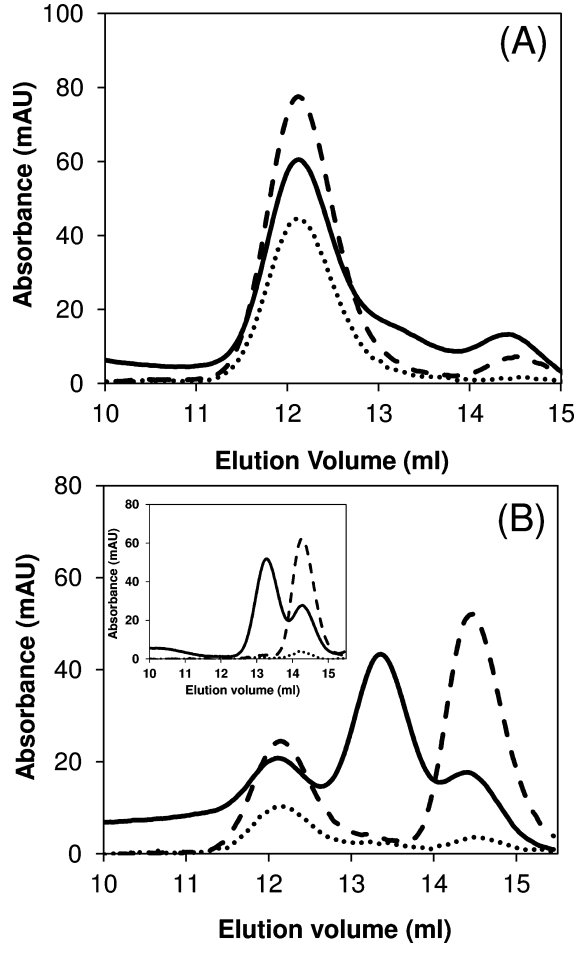

Figure 8. Gel filtration chromatograms of the solubilized NpHR in DDM after incubation at 45 °C for 24 h in the presence of 300 mM NaCl (A) or in the absence of NaCl (B). The elution profiles were monitored at 280 nm (solid line), 504 nm (dashed line), and 578 nm (dotted line). Inset: solubilized NpHR in Triton X-100 after incubation at 45 °C for 2 h in the absence of NaCl. The elution profiles were monitored at 280 nm (solid line), 504 nm (dashed line), and 578 nm (dotted line). Buffer conditions for gel filtration chromatography: 50 mM NaPi (pH 7.0) with 0.1% DDM and 150 mM NaCl.

trimeric NpHR and the BR has been retained in DDM even after heat treatment at 45 °C for 24 h in the presence of 300 mM NaCl. The same result was obtained in the case of solubilized complex in Triton X-100 (data not shown),

dx.doi.org/10.1021/bi201876p | *Biochemistry* 2012, 51, 2785–2794

indicating the strong intermolecular interactions between the NpHRs and/or the NpHR and the BR. Contrary to this, an increase in the peak intensity of $Abs_{280\ nm}$ at around 13.3 mL accompanied by a decrease in the peak intensity at 12.1 mL was caused by heat treatment at 45 °C in the desalted condition (Figure 8B, solid line). The molecular weight of the solubilized component with elution peak at 13.3 mL was calculated to be 100 kDa (Figure 6B (open circle)). It has been previously reported that trimeric ENpHR solubilized in DDM is dissociated to the monomer by heat treatment in the desalted condition;[15,16] in this study, the elution peak and molecular weight of the DDM−ENpHR monomer complex was 13.0 mL and 117 kDa, respectively (Figure 6B (open diamond)), close to those of the DDM−NpHR after heat treatment in the desalted condition. These results clearly indicate that the trimer NpHR in detergent dissociates to the monomer in a similar manner to the ENpHR. A little difference between the apparent molecular weights of DDM−NpHR and DDM−ENpHR may be caused, at least in part, by an effect of histidine tag bound to the ENpHR. This DDM−NpHR monomer complex with elution peak at 13.3 mL had no absorbance at 578 nm, reflecting the bleaching of the protein (Figure 8B, dotted line). Interestingly, the elution peak of the BR corresponding to $Abs_{504\ nm}$ was further moved to around 14.5 mL (dashed line). The elution peak of $Abs_{280\ nm}$ from the BR was also observed at 14.5 mL (solid line). Because this peak position reflects the unbound BR to the NpHR as shown in Figure 5, it is indicated that trimer dissociation of the NpHR is accompanied by the dissociation of the BR from the protein. In the case of the NpHR solubilized in Triton X-100, those dissociations have been occurred more rapidly and completely (Figure 8B, inset).

Binding Affinity for Cl^- and Resistance for Hydroxylamine of Solubilized NpHR−BR Complex. We examined the influence on the binding affinity for Cl^- of the NpHR−BR complex by solubilization. Figure 9 (inset) shows the difference spectra of the NpHR−BR in DDM titrated using NaCl. Obtained absorbance changes at around 630 nm accompanied by addition of NaCl are plotted in the Figure 9. As a result of fitting the data by the equation $\Delta A/\Delta A_{max} = [anion]^n/[(K_d)^n + [anion]^n]$, the dissociation constant K_d and Hill coefficient n were calculated to be 3.5 mM and 1.1 in the case of solubilized NpHR−BR (circles). These values were close to those of the NpHR−BR complex on the *N. pharaonis* membrane, 1.9 mM and 1.1 (triangles), indicating that the influence on the Cl^- binding affinity of NpHR by solubilization is minor.

The resistance to hydroxylamine under light illumination was also compared between the NpHR−BR complexes in DDM and on the membrane. Figure 10 shows the time course of the absorption decrease at 578 nm by 500 mM hydroxylamine under light illumination for NpHRs in the solubilized state (open triangles) and on the membrane (circles). Because the trimer NpHR has a high resistance basically, it needed the high hydroxylamine concentration (500 mM) to observe the photobleaching phenomenon. As a result, time constants for the photobleaching of the solubilized NpHR and the NpHR on the membrane were both about 3.3×10^{-5} s^{-1}. That is, both NpHRs had similar resistances to hydroxylamine. Contrary to this, bRs before and after solubilization had much different resistances to 50 mM hydroxylamine as shown in Figure 10 (inset); the time constant for photobleaching of the solubilized bR (2.6×10^{-3} s^{-1}) (circles) was about 150 times higher than that of bR on the purple membrane (1.7×10^{-5} s^{-1}) (triangles). From these results, it is suggested that the high resistance to hydroxylamine independent to the solubilization treatment is specific feature of the trimer NpHR.

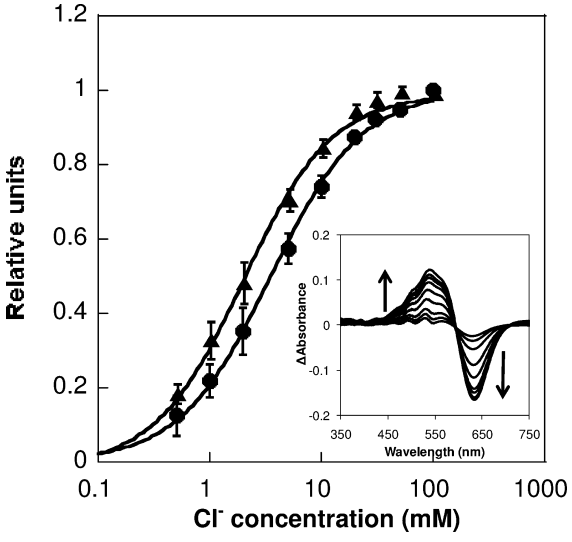

Figure 9. Absorbance change at around 630 nm vs Cl^- concentration during the $NpHR^{blue}$ to $NpHR^{Cl}$ reaction. Circles: solubilized NpHR−BR complex by DDM; triangles: NpHR on the *N. pharaonis* membrane. Inset: difference spectra of the solubilized NpHR−BR complex between the absorption spectra in the presence (0.5, 1, 2, 5, 10, 20, 30, 50, and 100 mM) and absence of Cl^-. Average values ± SD (n = 3). Correlation coefficients for the curve fittings were >0.99, respectively. Buffer conditions: 10 mM MOPS (pH 7.0).

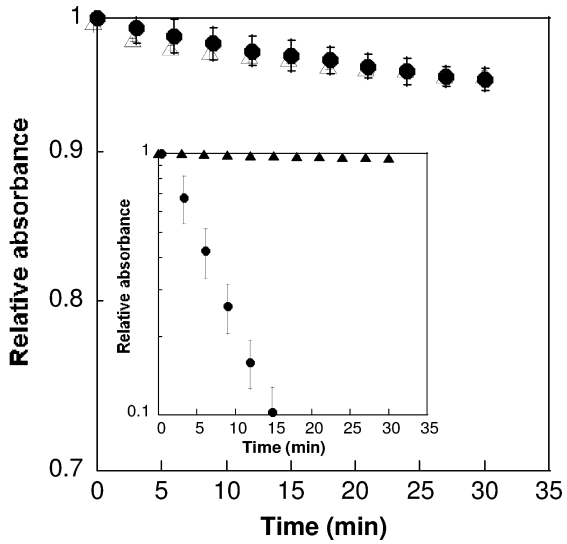

Figure 10. Time course of bleaching of NpHR by 500 mM hydroxylamine under light illumination (light intensity of 150 W) at 25 °C. Circles: solubilized NpHR−BR complex in DDM; open triangles: NpHR on the *N. pharaonis* membrane. Inset: time course of bleaching of bR by 50 mM hydroxylamine under light illumination at 25 °C. Circles: solubilized bR in Triton X-100; triangles: bR on the purple membrane. Average values ± SD (n = 3). Correlation coefficients for the curve fittings were >0.99, respectively. Buffer conditions: 10 mM MOPS (pH 7.0) with 150 mM NaCl.

dx.doi.org/10.1021/bi201876p | *Biochemistry* 2012, 51, 2785−2794

DISCUSSION

Structural Features of NpHR−BR Complex in the Solubilized System. In this study, a gel filtration chromatography monitored at 280 nm and SDS-PAGE clarified that NpHR solubilized from the biomembrane of the mutant strain KM-1 of *N. pharaonis* has retained its trimeric structure (Figures 6B and 7). Because the NpHR molecules in the solubilized system were cross-linked by glutaraldehyde that cross-links preferentially between the ε-amino groups of Lys, it is suggested that NpHRs have kept the configuration of the trimer as shown in Figure 1. In addition, the chromatogram monitored at $Abs_{578\ nm}$ which reflects the active state of NpHR had almost 100% of the peak area at the elution peak of 12.1 mL (Figure 4), indicating that almost all of the solubilized NpHRs with active state form the trimer. Further simultaneous monitoring at $Abs_{280\ nm}$ and $Abs_{504\ nm}$ characteristic to the protein and BR enabled to confirm clearly the NpHR−BR complex formation in the solubilized system (Figure 4).

A tight binding ability of the BR to the ENpHR trimer in the solubilized system has enabled the BR titration experiment (Figure 5A,B). As a result of this titration, it was revealed that the absorption peak ratio of $Abs_{578\ nm}$:$Abs_{504\ nm}$ = 1:2.5 is corresponding to the molar ratio of ENpHR:BR = 1:1 on the ENpHR−BR complex. These results leads to a conclusion that the solubilized NpHR−BR complex from *N. pharaonis* membrane with $Abs_{578\ nm}$:$Abs_{504\ nm}$ = 1:2.4 (Figure 3A) also has almost 1:1 of the binding ratio. However, there were some cases where the solubilized complexes have $Abs_{578\ nm}$:$Abs_{504\ nm}$ = 1:2.0−2.2 in our experimental condition. In fact, the ratio was 1:2.2 on the solubilized sample used in Figure 2A. One plausible idea for this variation is the effect of cultural condition of *N. pharaonis*. It has been reported by El-Sayed et al. that the synthesis of the BR by a halophilic archaea *H. salinarum* which also expresses halorhodopsin is reduced in the dark and low oxygen conditions.[30] In those cultural conditions, NpHR oligomers which have partially lacked the BR may be formed on the biomembrane with low BR content. In any case, it has been revealed that the NpHR trimer can exist at the molar ratio of NpHR:BR = 1:1 even in the solubilized state.

Solubilized NpHRs in DDM or Triton X-100 have retained the trimer structure even at high temperature condition of 45 °C as long as 300 mM NaCl has been contained in the solution (Figure 8A). This result reflects the strong intermolecular interactions between NpHRs. Contrary to this, trimeric NpHR was dissociated to the monomer by incubation at 45 °C in the absence of NaCl (Figure 8B); the same tendency has been observed in the case of ENpHR solubilized from *E. coli* membrane.[16] These results indicate that the ion binding to the NpHR is important to retain its oligomeric structure, and this change of the strength of trimeric association dependent on the NaCl is the universal nature for NpHR. Although the location of the ion binding site related to this trimeric association has not been identified yet, it is reported that the site has an affinities for Cl^- and SO_4^{2-} with dissociation constants of 22 and 94 mM, respectively.[16]

The dissociation of the NpHR trimer in the absence of NaCl also accompanied the dissociation of the BR from the NpHR−BR complex at the same time (Figure 8B). This result indicates that the cavity formed by the NpHR protomers in the trimeric conformation is important for binding of the BR. It is proposed from the X-ray crystal structure that the hydrogen bonds between the terminal polar groups of BR and Thr56 in one subunit and Glu197 in the adjacent subunit, and packing interactions between BR and helices A/B of one subunit and helices D/E of the adjacent subunit, are essential to the binding of the BR to the NpHR.[18] Disruption of these intermolecular interactions by the trimer dissociation of the NpHR is thought to be involved in the dissociation of the BR. In the case of xanthorhodopsin bound a carotenoid salinixanthin on the *Salinibacter ruber* membrane, it is also confirmed the preservation of the protein−carotenoid complex after solubilization by low concentration of DDM (0.15%).[9,31] However, the geometry of the salinixanthin is considerably different from that of the BR; the binding site of salinixanthin is the outer surface of helix F of the xanthorhodopsin and independent of the cavity formation by the protein.[10] So it may be the different carotenoid binding mechanisms between NpHR and xanthorhodopsin.

In the present study, increasing the thermal stability of the NpHR trimer conformation by binding of the BR was also observed; although only about 35% of the ENpHRs have retained the trimer after heat treatment (for 3 h at 45 °C in the absence of NaCl), almost all the ENpHR−BR complexes have retained the trimer even after the treatment (Figure 11).

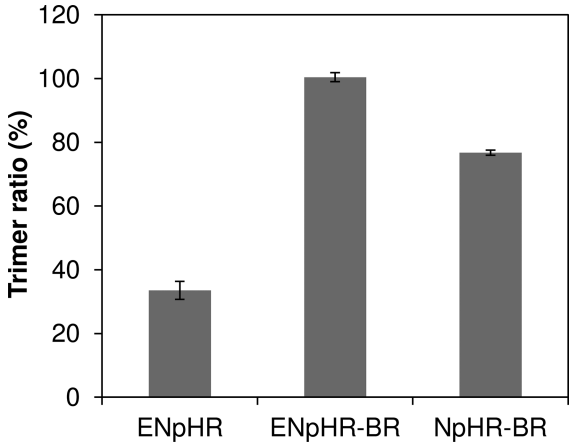

Figure 11. Trimer ratios of the solubilized ENpHR, solubilized ENpHR−BR, and solubilized NpHR−BR from *N. pharaonis* membrane after heat treatment at 3 h at 45 °C in the desalted condition. Average values ± SD (n = 3). Buffer conditions: 10 mM MOPS (pH 7.0).

These results suggest the physiological role of the BR to stabilize the trimer structure by binding to the crevice between the NpHR molecules, and dissociation of the BR may triggers the trimer dissociation of the NpHR. The NpHR−BR complex solubilized from the *N. pharaonis* membrane also had the stable trimer structure compared to the ENpHR. However, about 25% of the NpHR molecules were dissociated to the monomers (Figure 11). The principal difference between the trimer NpHRs obtained from *E. coli* and *N. pharaonis* membranes is the bound lipids to those; in the case of the trimer NpHR from *N. pharaonis* membrane, some phospholipids and other specific lipids are located in the center of the trimer.[18] It is thought that these archaeal lipids, which are not contained in the trimer ENpHR, are involved in a lower stability of the trimer NpHR−BR compared to the trimer ENpHR−BR.

Influence on the Local Structure and Function of NpHR by Solubilization. In the case of bR that forms a trimer and a further two-dimensional hexagonal lattice on the

dx.doi.org/10.1021/bi201876p | *Biochemistry* 2012, 51, 2785−2794

purple membrane, the strong and specific interprotein/protein−lipid interactions in the lattice structure lead to the high resistance of the bR to DDM.[32] When those interactions are disrupted by solubilization using octyl-β-D-glucoside or Triton X-100 which have higher solubilization abilities than DDM, the local structural change of the bR is observed spectroscopically and as a change of protein stability. That is, (1) blue shift of λ_{max} by about 12 nm,[33,34] (2) remarkable decrease in the resistance to hydroxylamine under illumination (Figure 10), and (3) decrease in the thermal stability of the protein molecule.[28,35] Contrary to this, as shown in Figure 2B, NpHR trimer on the *N. pharaonis* membrane in the presence of 100 mM NaCl was easily solubilized not only by Triton X-100 but also by DDM. These results suggest that the lipid-mediated intertrimer interaction of the NpHRs on the membrane is weak. The influence on the local structure of the NpHR accompanied by solubilization was also small. For instance, λ_{max} of the NpHR in both the presence (578 nm) and absence (600 nm) of NaCl (Figure 3A,B), and the resistance to hydroxylamine (Figure 10), were almost not changed by solubilization from the membrane. The change of binding affinity for Cl^- was also minor (Figure 9). Inversely, intermolecular interactions within the NpHR trimer in the presence of Cl^- is thought to be very strong because the NpHR has retained the trimer even after solubilization treatment by Triton X-100 (Figure 6A (dashed line)) which solubilizes the bR to the monomer.[27−29] Moreover, the BR molecules in the NpHR−BR complexes were also hardly dissociated from the NpHR trimers by detergent treatment in the presence of Cl^- (Figure 4), supporting the idea that the intermolecular interactions between the NpHRs and/or the NpHR and the BR in the complex is strong.

Because many other 7TMs known to form oligomer and/or crystalline array like as rhodopsin and halorhodopsin from *H. salinarum* are also solubilized to a monomeric level in the high concentration of the nonionic detergent,[36,37] it is a unique characteristic for NpHR to retain the trimer rigidly in the solubilized system. It has been reported that the monomerized NpHR shows a remarkable decrease in the resistance to hydroxylamine under illumination and a rapid bleaching by desalting.[15,16] These reports and results in this study clearly indicate that the retaining the trimeric structure in the solubilized state contributes to keep the local structure of the retinal and the flexibility of the NpHR during the functional state like as that on the membrane.

In this way, the NpHR−BR complex in the solubilized system, which structure hardly changes compared to that on the biomembrane and can be controlled by NaCl concentration and heat, is a good model system to investigate the specific intermolecular interactions between the 7TMs and 7TM−lipid conveniently.

AUTHOR INFORMATION

Corresponding Author

*Fax: +81-44-934-7321; e-mail: tsasaki@isc.meiji.ac.jp.

Notes

The authors declare no competing financial interest.

ACKNOWLEDGMENTS

We thank Dr. Tsutomu Kouyama and Dr. Kunio Ihara (Nagoya University, Japan) for the generous gift of *N. pharaonis* strain KM-1 (DSM2160^T).

ABBREVIATIONS

NpHR, *N. pharaonis* halorhodopsin; ENpHR, *N. pharaonis* halorhodopsin expressed on the *E. coli* membrane; BR, bacterioruberin; bR, bacteriorhodopsin; DDM, *n*-dodecyl β-D-maltopyranoside; GA, glutaraldehyde.

REFERENCES

(1) Franco, R., Casadó, V., Cortés, A., Ferrada, C., Mallol, J., Woods, A., Lluis, C., Canela, E. I., and Ferré, S. (2007) Basic concepts in G-protein-coupled receptor homo- and heterodimerization. *TheScientificWorldJournal 7*, 48−57.

(2) Milligan, G. (2010) The role of dimerisation in the cellular trafficking of G-protein-coupled receptors. *Curr. Opin. Pharmacol. 10*, 23−29.

(3) Henderson, R., and Unwin, P. N. T. (1975) Three-dimensional model of purple membrane obtained by electron microscopy. *Nature 257*, 28−32.

(4) Shibata, M., Yamashita, H., Uchihashi, T., Kandori, H., and Ando, T. (2010) High-speed atomic force microscopy shows dynamic molecular processes in photoactivated bacteriorhodopsin. *Nat. Nanotechnol. 5*, 208−212.

(5) Mitchell, D. C., Niu, S.-L., and Litman, B. J. (2001) Optimization of receptor-G protein coupling by bilayer lipid composition I: kinetics of rhodopsin-transducin binding. *J. Biol. Chem. 276*, 42801−42806.

(6) Niu, S.-L., Mitchell, D. C., and Litman, B. J. (2001) Optimization of receptor-G protein coupling by bilayer lipid composition I: formation of metarhodopsin II-transducin complex. *J. Biol. Chem. 276*, 42807−42811.

(7) Grossfield, A., Feller, S. E., and Pitman, C. (2006) A role for direct interactions in the modulation of rhodopsin by ω-3 polyunsaturated lipids. *Proc. Natl. Acad. Sci. U. S. A. 103*, 4888−4893.

(8) Soubias, O., and Gawrisch, K. (2005) Probing specific lipid-protein interaction by saturation transfer difference NMR spectroscopy. *J. Am. Chem. Soc. 127*, 13110−13111.

(9) Balashov, S. P., Imasheva, E. S., Boichenko, V. A., Antón, J., Wang, J. M., and Lanyi, J. K. (2005) Xanthorhodopsin: A proton pump with a light-harvesting carotenoid antenna. *Science 309*, 2061−2064.

(10) Luecke, H., Schobert, B., Stagno, J., Imasheva, E. S., Wang, J. M., Balashov, S. P., and Lanyi, J. K. (2008) Crystallographic structure of xanthorhodopsin, the light-driven proton pump with a dual chromophore. *Proc. Natl. Acad. Sci. U. S. A. 105*, 16561−16565.

(11) Lanyi, J. K., and Balashov, S. P. (2008) Xanthorhodopsin: A bacteriorhodopsin-like proton pump with a carotenoid antenna. *Biochim. Biophys. Acta 1777*, 684−688.

(12) Bivin, D. B., and Stoeckenius, W. (1986) Photoactive retinal pigments in haloalkaliphilic bacteria. *J. Gen. Microbiol. 132*, 2167−2177.

(13) Váró, G. (2000) Analogies between halorhodopsin and bacteriorhodopsin. *Biochim. Biophys. Acta 1460*, 220−229.

(14) Sato, M., Kanamori, T., Kamo, N., Demura, M., and Nitta, K. (2002) Stopped-flow analysis on anion binding to blue-form halorhodopsin from *Natronobacterium pharaonis*: comparison with the anion-uptake process during the photocycle. *Biochemistry 41*, 2452−2458.

(15) Sasaki, T., Kubo, M., Kikukawa, T., Kamiya, M., Aizawa, T., Kawano, K., Kamo, N., and Demura, M. (2009) Halorhodopsin from *Natronomonas pharaonis* forms a trimer even in the presence of a detergent, dodectyl-β-D-maltoside. *Photochem. Photobiol. 85*, 130−136.

(16) Sasaki, T., Aizawa, T., Kamiya, M., Kikukawa, T., Kawano, K., Kamo, N., and Demura, M. (2009) Effect of chloride binding on the thermal trimer-monomer conversion of halorhodopsin in the solubilized system. *Biochemistry 48*, 12089−12095.

(17) Tsukamoto, T., Sasaki, T., Fujimoto, K. J., Kikukawa, T., Kamiya, M., Aizawa, T., Kawano, K., Kamo, N., and Demura, M. (2011) Homo-timer formation and dissociation of *pharaonis* halorhodopsin in detergent system. *Biophys. J.*,.

(18) Kouyama, T., Kanada, S., Takeguchi, Y., Narusawa, A., Murakami, M., and Ihara, K. (2010) Crystal structure of the light-driven chloride pump halorhodopsin from *Natronomonas pharaonis*. *J. Mol. Biol. 396*, 564−579.
(19) Kanada, S., Takeguchi, Y., Murakami, M., Ihara, K., and Kouyama, T. (2011) Crystal structure of an O-like blue form and an anion-free yellow form of *pharaonis* halorhodopsin. *J. Mol. Biol. 413*, 162−176.
(20) Ihara, K., Narusawa, A., Maruyama, K., Takeguchi, M., and Kouyama, T. (2008) A halorhodopsin-overproducing mutant isolated from an extremely haloalkaliphilic archaeon *Natronomonas pharaonis*. *FEBS Lett. 582*, 2931−2936.
(21) Scharf, B., and Engelhard, M. (1994) Blue halorhodopsin from *Natronobacterium pharaonis*: wavelength regulation by anions. *Biochemistry 33*, 6387−6393.
(22) Oesterhelt, D., and Stoeckenius, W. (1974) Isolation of the cell membrane of Halobacterium halobium and its fractionation into red and purple membrane. *Methods Enzymol. 31*, 667−678.
(23) Rehorek, M., and Heyn, M. P. (1979) Binding of all-trans-retinal to the purple membranes. Evidence for cooperativity and determination of the extinction coefficient. *Biochemistry 18*, 4977−4983.
(24) Kelly, M., Norgard, S., and Liaaen-Jensen, S. (1970) Bacterial Cartenoids. 31. C_{50}-Carotenoids 5. Carotenoids of *Halobacterium salinarum*, especially bacterioruberin. *Acta Chem. Scand. 24*, 2169−2182.
(25) Zhang, R., and Somasundaran, P. (2004) Abnormal micellar growth in sugar-based and ethoxylated nonionic surfactants and their mixtures in dilute regimes using analytical ultracentrifugation. *Langmuir 20*, 8552−8558.
(26) Yamashita, Y., Kikukawa, T., Tsukamoto, T., Kamiya, T., Aizawa, T., Kawano, K., Miyauchi, S., Kamo, N., and Demura, M. (2011) Expression of *salinarum* halorhodopsin in *Escherichia coli* cells: Solubilization in the presence of retinal yields the natural state. *Biochim. Biophys. Acta 1808*, 2905−2912.
(27) Reynolds, J. A., and Stoeckenius, W. (1977) Molecular weight of bacteriorhodopsin solubilized in Triton X-100. *Proc. Natl. Acad. Sci. U. S. A. 74*, 2803−2804.
(28) Gottschalk, M., Dencher, N. A., and Halle, B. (2001) Microsecond exchange of internal water molecules in bacteriorhodopsin. *J. Mol. Biol. 311*, 605−621.
(29) Sasaki, T., Sonoyama, M., Demura, M., and Mitaku, S. (2005) Photobleaching of bacteriorhodopsin solubilized with Triton X-100. *Photochem. Photobiol. 81*, 1131−1137.
(30) El-Sayed, S. M. W., Takaichi, S., Saida, H., Kamekura, M., Abu-Shady, M., Seki, H., and Kuwabara, T. (2002) Effects of light and low oxygen tension on pigment biosynthesis in *Halobacterium salinarum*, revealed by a novel method to quantify both retinal and carotenoids. *Plant Cell Physiol. 43*, 379−383.
(31) Balashov, S. P., Imasheva, E. S., and Lanyi, J. K. (2006) Induced chirality of the light-harvesting carotenoid salinixanthin and its interaction with the retinal of xanthorhodopsin. *Biochemistry 45*, 10998−11004.
(32) Sasaki, T., Demura, M., Kato, N., and Mukai, Y. (2011) Sensitive detection of protein-lipid interaction change on bacteriorhodopsin using dodecyl β-D-maltoside. *Biochemistry 50*, 2283−2290.
(33) Dencher, N. A., and Heyn, M. P. (1978) Formation and properties of bacteriorhodopsin monomers in the non-ionic detergents octyl-b-D-glucoside and Triton X-100. *FEBS Lett. 96*, 322−326.
(34) Meyer, O., Ollivon, M., and Patemostre, M. T. (1992) Solubilization steps of dark-adapted purple membrane by Triton X-100. A spectroscopic study. *FEBS Lett. 305*, 249−253.
(35) Mukai, Y., Kamo, N., and Mitaku, S. (1999) Light-driven denaturation of bacteriorhodopsin solubilized by octyl-β-D-glucoside. *Protein Eng. 12*, 755−759.
(36) Kota, P., Reeves, P. J., RajBhandary, U. L., and Khorana, H. G. (2006) Opsin is present as dimers in COS1 cells: identification of amino acids at the dimeric interface. *Proc. Natl. Acad. Sci. U. S. A. 103*, 3054−3059.
(37) Hasselbacher, C. A., Spudich, J. L., and Dewey, T. G. (1988) Circular dichroism of halorhodopsin: comparison with bacteriorhodopsin and sensory rhodopsin I. *Biochemistry 27*, 2540−2546.